PCCR^{+}: Leveraging Pupil Dynamics for Correcting PCCR Slippage Error

Diako Mardanbegi

Google, Canada

Abstract. Head-mounted eye tracking is pivotal for extended reality but suffers from mechanical slippage. Unlike model-based approaches, regression-based Pupil Center-Corneal Reflection (PCCR) methods are not very robust against sensor displacement as they discard absolute geometric information of the eye features. This paper presents PCCR^{+}, a dynamic correction method that leverages absolute pupil dynamics to mitigate slippage error. A correction term is introduced, derived from the discrepancy between absolute pupil estimates and relative PCCR estimates. Utilizing a secondary "slip-calibration", a mapping is established between the PCCR vector and a dynamic gain coefficient. Simulation evaluations demonstrate that PCCR^{+}reduces mean absolute error by approximately 82% compared to the conventional PCCR method. While empirical validation remains for future work, this theoretical framework establishes a robust mathematical foundation for mitigating slippage errors in off-the-shelf solutions, without necessitating the complex geometric reconstruction required by model-based approaches.

Keywords: eye tracking · user interfaces · human-computer interaction

1 Introduction

The term 'PCCR' (Pupil Center-Corneal Reflection) is sometimes used to describe any gaze estimation method that uses pupil and corneal reflection (glint) centers; however, the term is more commonly associated with regression-based methods that use the vector connecting the pupil center to the glint center directly as input, mapping it to a gaze output via a regression function. This is distinct from 3D Model-Based methods, which utilize pupil and/or glint features to estimate the eye center, corneal center, and ultimately the gaze direction.

The classic Pupil-Center Corneal-Reflection method operates under the assumption that minor head movements cause both the pupil and the corneal glint to shift equally in the camera image. Consequently, the vector connecting them remains constant relative to the user's gaze angle. A practical demonstration of this concept is observing the eye of another person as they fixate on a light source while translating their head; the relative positions of the glint and the pupil remain largely unchanged. The PCCR approach was originally developed based on this principle for remote, screen-based eye tracking, where the three key components (the camera, the light source, and the display) are located on a fixed table. However, this principle is often invalid for head-mounted eye-tracking systems. Head-mounted eye trackers can be categorized into four types based on their gaze estimation output:

1. Head-mounted eye trackers that estimate gaze as (x, y) coordinates in the camera image.
2. Those that estimate gaze as (x, y) coordinates on a remote, world-fixed screen.
3. Those that estimate gaze as (x, y) coordinates on a head-fixed display (e.g., HMD).
4. Those that estimate gaze as an (x, y, z) vector or point in the 3D headset coordinate system.

The primary focus of this paper is on the fourth type. A correction approach to the PCCR method is proposed, demonstrating how a correction term derived from absolute pupil position can significantly improve the accuracy of the PCCR method during large device slippage. The correction method described in this paper may also apply to the other categories. Nevertheless, the parallax between the fixation point on the display and the camera in Type 3 and the shift of the front-facing camera in Type 1 may introduce complications that must be taken into account. The main motivation for the proposed correction method stems from the fact that PCCR discards information regarding the absolute position of the eye features. Instead, it utilizes the pupil-glint vector as a relative input, which does not necessarily remain invariant during slippage while the user maintains fixation on a world-fixed point.

Consider a near-eye eye-tracking system that estimates gaze as a 3D vector originating from a nominal eye center fixed within the headset's coordinate system. When the glasses slip downward while the user maintains fixation on a stationary world point, the sensors and light sources shift relative to the eye. Consequently, the tracker—referencing the now-displaced nominal eye center—interprets the altered pupil-glint geometry as an upward gaze shift. While the downward translation of the frame and the apparent upward rotation of the gaze vector might intuitively seem to counterbalance, the resulting geometry is non-trivial, particularly when factoring in variable target depths and complex multi-axis slippage.

The primary contribution of this paper is the derivation of a pupil-based correction term for the PCCR method. It is acknowledged that modern eye tracking has largely transitioned to model-based or machine-learning approaches, which currently offer superior practical robustness in commercial applications. However, deriving a closed-form geometric solution for PCCR slippage provides essential theoretical completeness to the classical method, without claiming competitive commercial performance. Therefore, this paper focuses exclusively on the theoretical derivation and idealized simulated validation of this correction term, establishing a mathematical baseline prior to real-world hardware deployment.

2 Related Work

Although the PCCR method's sensitivity to head movement is documented in the literature [7, 9], there is a lack of systematic research regarding the specific impact of slippage on PCCR accuracy in head-mounted eye tracking. Existing works, such as Hua et al. [6], offer only theoretical justifications suggesting that differential feature movement can isolate slippage, without providing experimental validation of PCCR accuracy under these conditions. Niehorster et al. demonstrated that natural behaviors, such as speaking and facial expressions, introduce slippage that can significantly degrade data quality, increasing gaze deviation by 0.8°–3.1° across multiple head-worn systems [10]. However, to the best of our knowledge, none of those glasses tested were operating based on the PCCR regression method.

Guestrin and Eizenman mathematically demonstrated that gaze estimation systems utilizing a single camera and single light source are inherently underdetermined, producing only 13 scalar equations for 14 unknowns. They showed that without external constraints such as a fixed head or independent depth estimation, it is impossible to uniquely distinguish between eye rotation and head translation [4]. While Guestrin and Eizenman specifically discuss head translation in a remote setup, the mathematical problem they identify is identical and geometrically isomorphic to headset slippage in a mobile setup.

Over the past decades, numerous model-based gaze estimation methods have been proposed, employing various configurations of cameras and light sources to reconstruct 3D eye geometry (e.g., [5, 14, 4]) and even glint-free approaches such as [11]. Unlike classic regression-based PCCR methods which rely on the pupil-glint vector and differ in their ability to mathematically distinguish eye rotation from sensor translation, model-based approaches aim to explicitly solve for these geometric shifts. While model based approaches provide higher degrees of robustness against slippage, they have to deal with geometrical problems such as solving for cornea and eye center, modeling pupil refraction, estimating person's kappa angle (visual-optical axes offset) and other subjective difference such as cornea radius and pupil offset from cornea center [15].

Several works have studied the effect of model choice on PCCR accuracy [3, 8, 2]. Mardanbegi et al. demonstrated that while 3rd-order polynomials improve wide-angle accuracy, they are more prone to extrapolation errors at the edges than 2nd-order models in mobile eye trackers [8].

Sesma-Sanchez et al. (2012) evaluated interpolation-based methods using binocular data, finding that normalizing pupil-glint vectors with interglint distance significantly improves robustness against head movements. Additionally, they demonstrated that averaging the estimated gaze from both eyes generally yields higher accuracy and stability compared to single-eye estimation, particularly when error differences between eyes are minimal [12].

Narcizo et al. (2021) proposed geometric transformations to improve interpolation-based gaze estimation by correcting for camera displacement and the non-coplanarity error caused by spherical eye rotation. Although they demonstrated that virtually realigning the eye feature distribution mitigates errors caused by camera misalignment, their experimental validation relied entirely on remote desktop trackers rather than head-mounted displays [9]. Others have also looked at post-calibration corrections to improve the PCCR nonlinearity problem [1].

3 PCCR^{+}Method

The PCCR^{+}method fuses gaze estimation obtained from absolute pupil position and PCCR vector using a learned, spatially varying gain coefficient. This allows the system to rely on the stability of the pupil-glint vector while correcting for the geometric errors introduced by headset slippage.

3.1 Rationale: PCCR vs Pupil Gaze

A mathematical description of the correlation between pupil gaze and PCCR gaze is not straightforward. It requires modeling several complex, interrelated factors, including the camera and the light source, the dynamic interaction between the glint reflection and the refracted pupil, and how these elements change in the image as slippage occurs.

This correlation was investigated using the simulation framework described in Section 4. Both the Pupil and PCCR methods were calibrated using 2nd-order polynomial regression across a 3x3 grid of $40° \times 30°$ deg. Post-calibration, the gaze estimation performance of both methods was evaluated across four specific targets: Center, Far Right, Top Right, and Top. The evaluation utilized the standard slip model described in Section 4, where slippage is modeled as a parameterized drift along the nasal dorsum (combining magnitude, angle, and coupled pitch). For each target, 100 random slips were simulated with magnitudes ranging from 0 to 10 mm. While the fixation targets remained static in the world coordinate system, displacements were applied solely to the camera and light source positions according to the slip model. Gaze estimation was evaluated using azimuth and elevation angles, calculated relative to the ground truth vector defined by the nominal eye center and the fixed target positions in the headset coordinate system.

The plot in Figure 1 shows the correlation between PCCR gaze error and the discrepancy between PCCR and pupil gaze, indicating that the PCCR error correlates with pupil error. It is also important to note that this relationship changes depending on the gaze position. This suggests that the PCCR error can potentially be corrected to some extent by using a term that is a function of both PCCR gaze and pupil gaze. Specifically, the PCCR gaze determines the relevant slope, while the discrepancy between the PCCR and pupil estimates indicates the specific correction value required along that line.

3.2 Base Gaze Estimators

Let $\mathbf{x}_p = (u_p, v_p)$ denote the coordinates of the pupil center and $\mathbf{x}_g = (u_g, v_g)$ denote the coordinates of the glint in the camera image plane. We define the pupil-glint vector (PCCR vector) as $\mathbf{v}_{pccr} = \mathbf{x}_p - \mathbf{x}_g$.

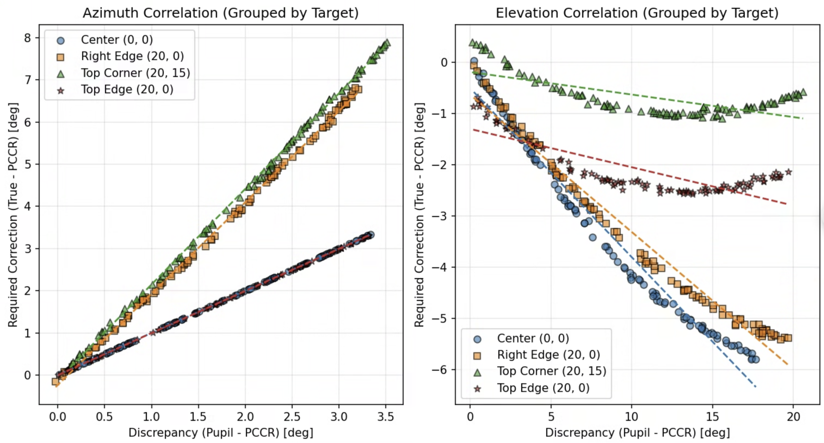

Fig. 1: Results from 100 random slips parameterized by the drift model comparing PCCR gaze error (vertical axis) with the discrepancy between PCCR and pupil gaze (horizontal axis). Samples are split into groups corresponding to the specific gaze targets.

Two distinct base gaze estimators are employed, both modeled as second-order multivariate polynomials that map feature vectors to horizontal and vertical gaze angles ($\mathcal{P}^2 : \mathbb{R}^2 \to \mathbb{R}^2$).

The pupil gaze estimator (f_{pupil}) maps the absolute pupil coordinates directly to gaze angles. While highly sensitive to headset shifts, it serves as the baseline anchor for our correction term. The PCCR gaze estimator (f_{pccr}), on the other hand, maps the relative vector $\mathbf{v}_{pccr}$ to gaze angles.

$$\hat{\mathbf{g}}_{pupil} = f_{pupil}(\mathbf{x}_p) \tag{1}$$

$$\hat{\mathbf{g}}_{pccr} = f_{pccr}(\mathbf{v}_{pccr}) \tag{2}$$

3.3 Dynamic Gain Correction

It is hypothesized that under slippage conditions, the true gaze direction g_{true} lies on the linear trajectory connecting the two base estimates $\hat{g}_{pccr}$ and $\hat{g}_{pupil}$. Consequently, the corrected gaze $\hat{g}_+$ can be formulated as the PCCR estimate adjusted by a weighted residual of the pupil estimate:

$$\hat{g}_+ = \hat{g}_{pccr} + K \odot (\hat{g}_{pupil} - \hat{g}_{pccr}) \tag{3}$$

where $\odot$ denotes element-wise multiplication, and $K = (k_{az}, k_{el})$ is a dynamic gain vector. To improve the model's ability to distinguish between downward gaze and forward glasses pitch, the vertical pupil position (y_{pupil}) is included as a context feature. Therefore, K is modeled as a learned function of both the PCCR vector and the absolute vertical pupil position:

$$K \approx \mathcal{M}_{gain}(v_{pccr}, y_{pupil}) \tag{4}$$

The model $\mathcal{M}_{gain}$ is implemented using Ridge regression with 2nd-order polynomial features to ensure stability against outliers.

3.4 Training the Gain Model

To train the model $\mathcal{M}_{gain}$, a dedicated training set distinct from the initial calibration grid is utilized, ideally containing samples with induced headset slippage. For each sample i in this set, the ideal target gain $\mathbf{K}_i^*$ is calculated to satisfy Eq. 3 given the ground truth gaze $\mathbf{g}_{true,i}$:

$$\mathbf{K}_i^* = \frac{\mathbf{g}_{true,i} - \hat{\mathbf{g}}_{pccr,i}}{\hat{\mathbf{g}}_{pupil,i} - \hat{\mathbf{g}}_{pccr,i}} \tag{5}$$

The division is performed element-wise. A 2nd-order polynomial regressor is then trained to map the input features $\mathbf{v}_{pccr}$ to the target gains $\mathbf{K}^*$. During inference, the system predicts $\mathbf{K}$ based on the current relative eye features and applies the correction described in Eq. 3.

3.5 Calibration Requirements

As discussed, a standard single-step calibration is insufficient because it typically contains near-zero slippage (and thus near-zero error). Therefore, this method relies on a secondary calibration ($\mathcal{C}_{\text{slip}}$) in addition to the nominal calibration ($\mathcal{C}_{\text{nominal}}$). The second calibration has to be done after the headset is physically shifted. This generates samples with high error ($\mathbf{y}$ is large). By using samples collected from these two sets, the method can learn the dynamic correction gain on the user. Note that the slip state should ideally represent a typical glasses shift along the nose.

4 Experimental Setup

4.1 Simulation

The numerical results in this study were generated using a high-fidelity eye tracking simulator. The simulation incorporates a spherical corneal model, glint reflections, and pupil refraction. The offset between the optical and visual axes (angle kappa) is not modeled, and the simulation assumes noise-free feature detection. These are intentional simplifications designed to isolate and validate the core geometric proof of the correction term, rather than to simulate a full deployment environment. Scleral glints are also ignored.

The simulated head-mounted eye tracking system consisted of a single camera and light source per eye. Two distinct configurations were defined for the system:

- CONFIG1: An ideal configuration with the camera and light source positioned directly in front of the eye (both at a distance of 30 mm, with the light source shifted 5 mm nasally).
- CONFIG2: Identical to CONFIG1, but with both components positioned 15 mm below the eye center.

The first configuration is used to investigate the correlation in an ideal setup and the second configuration, which is more realistic, is used to evaluate the proposed method. All the results in this paper are based on the data from a simulated binocular setup and the primary focus is on the accuracy of the combined gaze.

The fixation targets were defined on a fixed plane 100 cm away from the eye and the ground truth gaze vector is always calculated from the nominal eye center defined in the headset coordinate system (fixed with respect to the camera). Both f_{pupil} and f_{pccr} models are calibrated using a standard calibration sequence (e.g., a 9-point grid).

4.2 Modeling Drift Slippage

In this paper, slippage is modeled as a scalar drift s along the nasal dorsum. The trajectory is governed by the subject's Nasofacial Angle (α), defined as the angle between the nasal dorsum and the vertical facial plane. The resulting translation $\Delta\mathbf{t}$ (of the headset frame relative to the eye) and pitch rotation $\Delta\phi$ are defined as:

$$\Delta\mathbf{t} = s \cdot [0, -\cos\alpha, \sin\alpha]^\top, \quad \Delta\phi = \rho \cdot s \tag{6}$$

A biomechanical coupling was enforced where the glasses pitch forward as they slip down the nose. The pitch rotation ϕ was determined by the slip magnitude using a fixed coefficient ρ. This linear approximation decouples slip magnitude from user anatomy, allowing for efficient simulation of diverse morphological constraints.

For the Nasofacial Angle (α), anthropometric studies indicate a mean of approximately $32.4° \pm 3.3°$, with observed values spanning 25°–42° rather than a defined ideal range [16]. For the Pitch Coefficient (ρ), a nominal range of 0.5°–0.7°/mm is estimated. This is geometrically derived from the standard "Canthus-to-Tragus" distance (approx. 72mm) plus the orbital depth, creating an effective pivot radius of 85–90mm from the ear to the nasal bridge [13].

4.3 Experimental Design

Two separate experiments were designed to evaluate the proposed PCCR$^+$method using synthetic data generated from CONFIG2, which represents a more realistic setup where the eye camera and light source are positioned on the lower rim of the glasses frame.

Single Subject Evaluation To evaluate the baseline performance of the proposed method, an initial assessment was conducted on a single simulated "subject". In this context, a subject is defined by a specific geometric configuration (Nasofacial Angle $\alpha = 30°$ and Pitch Coefficient $\rho = 0.6°/\text{mm}$), rather than an anatomical eye model, as the same eye model was used across all simulations. The evaluation focused on the accuracy of the combined gaze estimation under four discrete slip magnitudes: 2 mm, 4 mm, 6 mm, and 10 mm.

Generalization Analysis To evaluate the generalization capability of the proposed method, a rigorous robustness analysis was conducted using a Monte Carlo simulation. A randomized test dataset consisting of $N = 315$ unique slip conditions was generated. These test conditions were created by simulating 15 random subjects (with random facial geometries defined by Nasofacial angle and Pitch coefficient) across 21 distinct slip magnitudes ranging from 0 to 10 mm.

In contrast to independent pitch randomization, a biomechanical coupling was enforced where the glasses pitch forward as they slip down the nose. The pitch rotation ϕ was determined by the slip magnitude using a fixed coefficient ρ randomly sampled from $[0.5, 0.7]°/\text{mm}$. This experimental design tests the method's ability to interpolate and extrapolate corrections across a physically consistent range of mechanical slippage and diverse subject geometries.

The method was evaluated using gain models learned from two distinct training configurations: a "Low Slip" condition (C_{3mm}, representing a 3 mm slip where the pitch is subject-specific, derived from $\phi = \rho \cdot 3$) and a "High Slip" condition (C_{8mm}, representing an 8 mm slip where $\phi = \rho \cdot 8$).

5 Results

5.1 Single Subject Evaluation

Figure 2 illustrates the error distribution and Mean Absolute Error (MAE) for both the baseline PCCR and the PCCR$^+$methods at the four evaluated slip magnitudes.

5.2 Generalization

Table 1 summarizes the results across varying degrees of headset slippage for the Monte Carlo simulation. The random test samples were categorized into three bins based on displacement magnitude: micro-slips (0–2 mm), moderate slips surrounding the primary training point (2–4 mm), and large slips (4–10 mm). Examining single-eye gaze accuracy revealed very similar results to cyclopean gaze in terms of both accuracy and relative improvement per eye.

The baseline PCCR method exhibits a significant degradation in accuracy as slippage increases, with errors reaching 7.97° in the largest bin (4–10 mm). In contrast, the PCCR$^+$method demonstrates strong generalization. The model trained on the 3 mm condition ($\mathcal{C}_{3\text{mm}}$) reduced the overall mean angular error

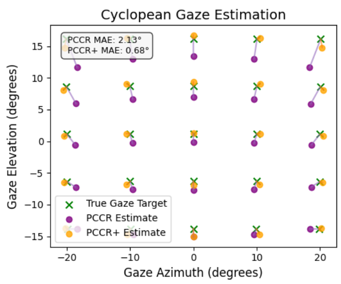

(a)

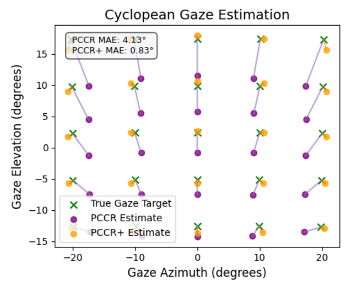

(b)

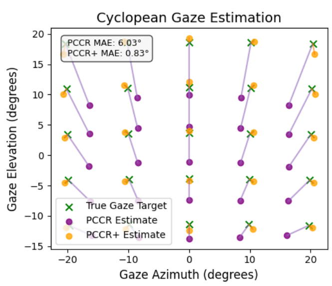

(c)

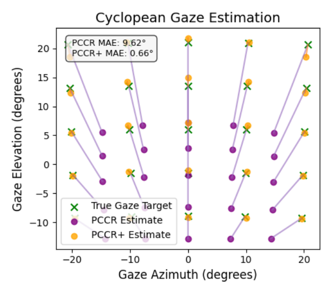

(d)

Fig. 2: Comparison of Mean Absolute Error (MAE) and error distribution for PCCR and PCCR$^+$methods at slip amplitudes of: (a) 2 mm, (b) 4 mm, (c) 6 mm, and (d) 10 mm

Table 1: Comparison of mean gaze estimation error (in degrees) grouped by headset slip magnitude. The PCCR$^+$method is evaluated using gain models learned from two distinct training configurations: C_{3mm} (trained on 3 mm slip) and C_{8mm} (trained on 8 mm slip).

Slip Magnitude	**PCCR** (Base)	**PCCR$^+$** ($\mathcal{C}_{3\text{mm}}$)	**PCCR$^+$** ($\mathcal{C}_{8\text{mm}}$)
Micro (0–2 mm)	1.40°	0.48°	0.58°
Training Range (2–4 mm)	3.88°	0.50°	0.78°
Large (4–10 mm)	7.97°	1.33°	0.72°
Combined (0–10 mm)	**5.63°**	**0.97°**	**0.70°**

by approximately 82% (from 5.63° to 0.97°). Even when extrapolated to slips up to 10 mm, it constrained the average error to 1.33°. Similarly, the model trained on the 8 mm condition ($\mathcal{C}_{8\text{mm}}$) effectively mitigated errors across the entire range, yielding a comparable error of 0.72° in the largest bin, confirming that the learned gain function captures the fundamental geometry of the slip rather than overfitting to a specific magnitude. The Cumulative Distribution Function (CDF) of gaze estimation errors is presented in Figure 3a, further illustrating the performance improvement across the entire test set.

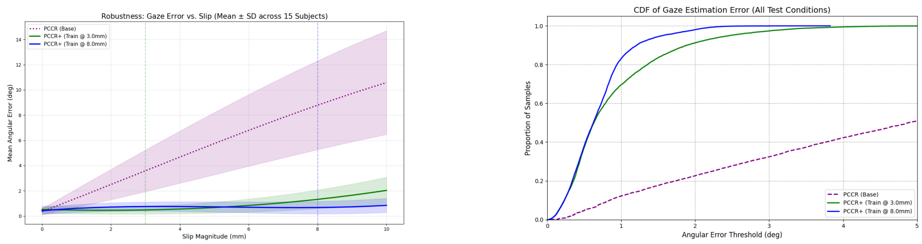

(a) (b)

Fig. 3: Results of testing the PCCR+ method on 315 random slip conditions with two different slip training configurations.

6 Limitations and Future Work

Although the correction term results in significant theoretical improvements in PCCR accuracy, a primary limitation of the proposed method is its dependence on a secondary calibration set to model user-specific slippage. Future research should investigate the feasibility of generalizing these coefficients to establish default parameters across users, alongside validation using real-world data.

Furthermore, the current validation relies on a noise-free, idealized simulation (e.g., assuming a spherical cornea and omitting angle kappa). In real-world environments, feature detection noise will inevitably impact the convergence and stability of the Ridge regression used to estimate the dynamic gain coefficient. Future empirical studies are essential to evaluate the algorithm's robustness against realistic sensor noise and complex biomechanical movements beyond the linear nasal drift modeled here.

7 Conclusion

In this paper, PCCR$^+$, a dynamic slip correction method for classic regression-based PCCR method tailored for mobile eye tracking, was introduced. The proposed gain correction method reduces slippage error by using a data-driven prior (the second calibration). The slippage error is approximated based on the correlation between the gaze errors obtained from pupil only and PCCR gaze outputs. The idealized simulation demonstrated that the correction term can theoretically reduce the mean absolute error by 82%. While real-world validation remains a necessary next step, this theoretical framework serves as a valuable conceptual enhancement for off-the-shelf mobile eye trackers that rely on PCCR regression, proving that the fusion of absolute and relative pupil metrics can systematically mitigate mechanical slippage.

Acknowledgements We dedicate this work to the memory of our colleague, Andrew Yang. We are deeply grateful for his foundational contributions in developing the eye-tracking simulation framework later utilized in this study. We also acknowledge his efforts in implementing a variation of this method on the Mindlink Eye Tracking glasses (AdHawk Microsystems, Waterloo, Canada), which established the vital groundwork for its future real-world validation.

References

1. Blignaut, P., Holmqvist, K., Nyström, M., Dewhurst, R.: Improving the accuracy of video-based eye tracking in real time through post-calibration regression. In: Current trends in eye tracking research, pp. 77–100. Springer (2013)
2. Cerrolaza, J.J., Villanueva, A., Cabeza, R.: Taxonomic study of polynomial regressions applied to the calibration of video-oculographic systems. In: Proceedings of the 2008 symposium on Eye tracking research & applications. pp. 259–266 (2008)
3. Cerrolaza, J.J., Villanueva, A., Cabeza, R.: Study of polynomial mapping functions in video-oculography eye trackers. ACM Transactions on Computer-Human Interaction (TOCHI) **19**(2), 1–25 (2012)
4. Guestrin, E.D., Eizenman, M.: General theory of remote gaze estimation using the pupil center and corneal reflections. IEEE Transactions on biomedical engineering **53**(6), 1124–1133 (2006)
5. Hennessey, C., Noureddin, B., Lawrence, P.: A single camera eye-gaze tracking system with free head motion. In: Proceedings of the 2006 symposium on Eye tracking research & applications. pp. 87–94 (2006)
6. Hua, H., Krishnaswamy, P., Rolland, J.P.: Video-based eyetracking methods and algorithms in head-mounted displays. Optics Express **14**(10), 4328–4350 (2006)
7. Jung, D., Lee, J.M., Gwon, S.Y., Pan, W., Lee, H.C., Park, K.R., Kim, H.C.: Compensation method of natural head movement for gaze tracking system using an ultrasonic sensor for distance measurement. Sensors **16**(1), 110 (2016)
8. Mardanbegi, D., Kurauchi, A.T., Morimoto, C.H.: An investigation of the distribution of gaze estimation errors in head mounted gaze trackers using polynomial functions. Journal of Eye Movement Research **11**(3), 10–16910 (2018)
9. Narcizo, F.B., Dos Santos, F.E.D., Hansen, D.W.: High-accuracy gaze estimation for interpolation-based eye-tracking methods. Vision **5**(3), 41 (2021)
10. Niehorster, D.C., Santini, T., Hessels, R.S., Hooge, I.T., Kasneci, E., Nyström, M.: The impact of slippage on the data quality of head-worn eye trackers. Behavior research methods **52**(3), 1140–1160 (2020)

11. Santini, T., Niehorster, D.C., Kasneci, E.: Get a grip: Slippage-robust and glint-free gaze estimation for real-time pervasive head-mounted eye tracking. In: Proceedings of the 11th ACM symposium on eye tracking research & applications. pp. 1–10 (2019)
12. Sesma-Sanchez, L., Villanueva, A., Cabeza, R.: Gaze estimation interpolation methods based on binocular data. IEEE transactions on biomedical engineering **59**(8), 2235–2243 (2012)
13. Talaat, W., McGraw, T., Klitzman, B.: Relationship between the canthal–tragus distance and the puncture point in temporomandibular joint arthroscopy. International journal of oral and maxillofacial surgery **39**(1), 57–60 (2010)
14. Villanueva, A., Cabeza, R.: A novel gaze estimation system with one calibration point. IEEE Transactions on Systems, Man, and Cybernetics, Part B (Cybernetics) **38**(4), 1123–1138 (2008)
15. Villanueva, A., Cerrolaza, J.J., Cabeza, R.: Geometry issues of gaze estimation. Advances in Human Computer Interaction p. 513 (2008)
16. Yilmaz, N.P.C., Bay, C., Yılmaz, I.N., Kelsaka, O., Ok, F.N., Ateş, A., Demirtas, E., Tekdemır, İ.: Unlocking nasal angle anthropometry and nasolabial angle preferences: a key to achieve the perfect rhinoplasty. Anatomy **17**(2), 70–81 (2023)